anticipate that the qualitative effects we have demonstrated in this paper will be unchanged.

References and Notes

(1) Stein, R. S.; Murray, C. T.; Yang, H.; Soni, V.; Lo, R. J. *Physica B* **1986**, *137*, 194. Wignall, G. D. *Encycl. Polym. Sci. Eng.* **1987**, *10*, 112.
(2) Wignall, G. D.; Crist, B.; Russell, T. P.; Thomas, E. L. Scattering, Deformation, and Fracture in Polymers. *Proc. MRS Symp.* **1987**, 79.
(3) Flory, P. J. *Principles of Polymer Chemistry*; Cornell University, Ithaca, NY, 1953.
(4) For reviews see: (a) Paul, D. R.; Barlow, J. W. In *Polymer Compatibility and Incompatibility*; Solc, K., Ed.; MMI Press: Midland, MI, 1981; p 1. (b) Sanchez, I. C. *Polymer Compatibility and Incompatibility*; MMI Press: Midland, MI, 1981; p 59. (c) Sanchez, I. C. *Ann. Rev. Mater. Sci.* **1983**, *13*, 387.
(5) Bates, F. S.; Koehler, W. C.; Wignall, G. D.; Fetters, L. J. Reference 2, p 159.
(6) Ito, H.; Russell, T. P.; Wignall, G. D. *Macromolecules* **1987**, *20*, 2214.
(7) Yang, H.; O'Reilly, J. M. Reference 2, p 129.
(8) Trask, C. A.; Roland, C. M. *Macromolecules* **1989**, *22*, 256.
(9) Schweizer, K. S.; Curro, J. G. *Phys. Rev. Lett.* **1987**, *58*, 246.
(10) Curro, J. G.; Schweizer, K. S. *Macromolecules* **1987**, *20*, 1928.
(11) Curro, J. G.; Schweizer, K. S. *J. Chem. Phys.* **1987**, *87*, 1842.
(12) Schweizer, K. S.; Curro, J. G. *Macromolecules* **1988**, *21*, 3070.
(13) Schweizer, K. S.; Curro, J. G. *Macromolecules* **1988**, *21*, 3082.
(14) Curro, J. G.; Schweizer, K. S.; Grest, G. S.; Kremer, K. *J. Chem. Phys.* **1989**, *91*, 1357.
(15) Chandler, D.; Andersen, H. C. *J. Chem. Phys.* **1972**, *57*, 1930.
(16) Chandler, D. In *Studies in Statistical Mechanics*; Montroll, E. W., Lebowitz, J. L., Eds.; North-Holland: Amsterdam, 1982; Vol. VIII, p 274 and references cited therein.
(17) Schweizer, K. S.; Curro, J. G. *Phys. Rev. Lett.* **1988**, *60*, 809.
(18) Curro, J. G.; Schweizer, K. S. *J. Chem. Phys.* **1988**, *88*, 7242.
(19) Schweizer, K. S.; Curro, J. G. *J. Chem. Phys.* **1989**, *91*, 5059.
(20) Bawendi, M. G.; Freed, K. F. *J. Chem. Phys.* **1988**, *88*, 2741.
(21) Bawendi, M. G.; Freed, K. F.; Mohanty, U. *J. Chem. Phys.* **1987**, *87*, 5534.
(22) Freed, K. F.; Pesci, A. I. *J. Chem. Phys.* **1987**, *87*, 5534.
(23) Flory, P. J. *J. Chem. Phys.* **1949**, *17*, 203.
(24) de Gennes, P.-G. *Scaling Concepts in Polymer Physics*; Cornell University Press: Ithaca, NY, 1979.
(25) Lowden, L. J.; Chandler, D. *J. Chem. Phys.* **1974**, *61*, 5228; **1973**, *59*, 6587; **1975**, *62*, 4246.
(26) Henderson, D. *Ann. Rev. Phys. Chem.* **1974**, *25*, 461.
(27) Kac, M.; Uhlenbeck, G.; Hemmer, P. D. *J. Math. Phys.* **1963**, *4*, 216.
(28) Schweizer, K. S.; Curro, J. G., in preparation.
(29) Paluka, T.; Geyler, S. *Macromolecules* **1988**, *21*, 1665.
(30) Cates, M. E.; Deutsch, J. M. *J. Phys. (Les Ulis, Fr.)* **1986**, *47*, 2121.
(31) Brereton, M. G.; Fischer, E. W.; Herkt-Maetzky, C.; Mortensen, K. *J. Chem. Phys.* **1987**, *87*, 6144.
(32) Curro, J. G.; Schweizer, J. G., in preparation.

Registry No. PMMA, 9011-14-7; PEO, 25322-68-3.

Physical Aging in Poly(methyl methacrylate)/ Poly(styrene-*co*-acrylonitrile) Blends. 3. Simulation of Enthalpy Relaxation Using the Moynihan Model

Tai Ho and Jovan Mijović*

Department of Chemical Engineering, Polytechnic University, 333 Jay Street, Brooklyn, New York 11201.

Received August 7, 1989; Revised Manuscript Received September 12, 1989

ABSTRACT: The Moynihan model was used to simulate enthalpy relaxation of a series of blends of poly(methyl methacrylate) (PMMA) with poly(styrene-*co*-acrylonitrile) (SAN). The optimized Moynihan parameters for each blend composition were obtained from the best fits of specific heat data in the glass transition region measured in the rate-heating approach experiments, whereby samples were reheated immediately after being cooled through the glass transition region. Optimization was carried out by using the Marquardt algorithm. The optimized parameters were then used in simulations of experiments following the isothermal approach, in which a period of isothermal relaxation was introduced between cooling and heating steps. Calculated values for the isothermal enthalpy relaxation agreed with previously reported experimental data within the margins of experimental uncertainty. The discrete formulation of the Moynihan model was meticulously constructed to ensure an accurate representation of that model.

Introduction

In the past 3 decades, researchers have devoted much effort to studying relaxation of glasses in the region which encompasses the glass transition and extends well into the glassy state. In that region, a change in temperature or the application of a small external mechanical load will cause time-dependent changes, or relaxation, in the structure, with concurrent changes in the properties of the material. Relaxation that leads to changes in the structure is referred to as structural relaxation, while the effect of relaxation under stress on properties of materials is one of the topics of viscoelasticity.[1]

Structural relaxation in polymers has been studied by following either volume relaxation[2,3] or enthalpy relaxation.[4-10] In Kovacs' classic work,[2,3,11] volume relaxation in organic glasses was found to be characterized by nonlinearity and nonexponentiality. Since volume relaxation is one of the many manifestations of structural relaxation, those two characteristics should also mark the structural relaxation of glasses in general. Moreover, Struik[12] has recently demonstrated that creep compliance of glasses also exhibits those characteristics. In a previous communication from our laboratory,[13] we have shown that the enthalpy relaxation of blends of poly-

* To whom correspondence should be addressed.

0024-9297/90/2223-1411$02.50/0

(methyl methacrylate) (PMMA) and poly(styrene-*co*-acrylonitrile) (SAN), measured with differential scanning calorimetry (DSC), is nonlinear.

In the past 2 decades, researchers have proposed various phenomenological models[4,5,11,14,15] to describe the structural relaxation phenomenon. A comprehensive review of those models is contained in a recently published book[1] and will not be repeated here. A phenomenological model describes the change of a certain property but does not provide a theoretical explanation for the observation. Instead, it serves an intermediate role, as it concisely presents the experimental data and provides a starting point for the development of a theory. In this study, one of the existing models for structural relaxation in the glassy state, namely, the Moynihan model,[4,5] was used to simulate the experimental results on enthalpy relaxation obtained by using both the rate-heating and the isothermal approach. The rate-heating approach, in which the specimen is cooled through the glass transition region and immediately heated back to the rubbery state, reveals the temperature dependence of the enthalpy relaxation, while the isothermal approach, which includes an isothermal period between cooling and heating, demonstrates both temperature and structure dependence of the relaxation. Also, in the isothermal approach, substantial structural change occurs during the isothermal period. The Moynihan model is chosen because of its frequent use as a model for structural relaxation.

A valid phenomenological model should be able to account for the results from experiments following either approach, and the ability to do so is herein referred to as "consistency". The primary objective of this work was to investigate the consistency of the Moynihan model by comparing calculated values and experimental data for enthalpy relaxation of a series of PMMA/SAN blends below the glass transition.

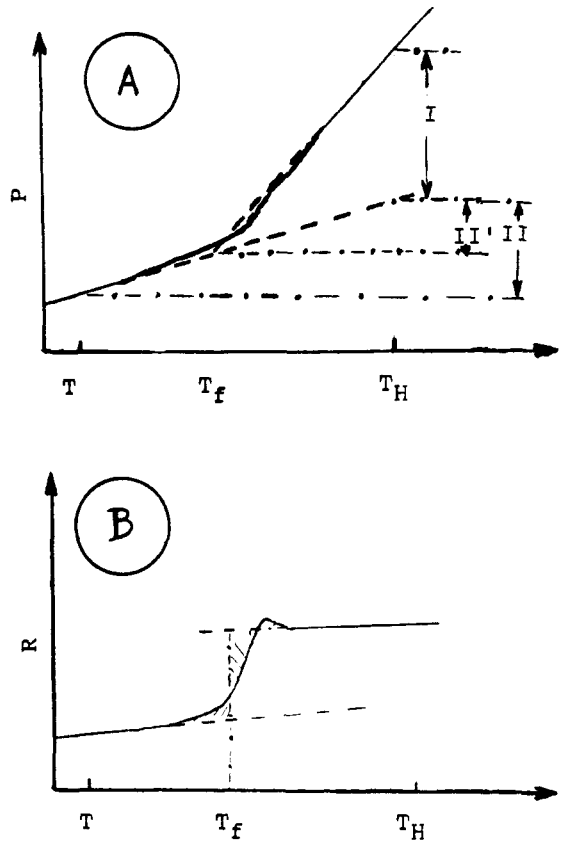

Figure 1. Schematic illustration showing property P and its temperature derivative R as functions of temperature; the position of the fictive temperature, T_f, is indicated in each diagram: plot A, P vs T; plot B, R vs T.

Theory

Structural Relaxation in Isothermal Conditions. Moynihan and co-workers reviewed investigations on isothermal relaxations of various properties following an instantaneous temperature change, or a temperature jump.[5] They found that an excellent fit of data was obtained by using the Williams–Watts equation[16] in the following form

$$\phi(t - t_1,t) = \frac{P - P_e}{P_0 - P_e} = \exp[-(\int_{t_1}^{t} dt'/\tau)^{\beta}] \qquad (1)$$

where

$$\tau = A \exp[X\Delta h^*/(RT) + (1 - X)\Delta h^*/(RT_f)] \qquad (2)$$

In eq 1, t_1 is the time when the change in temperature occurs, P_0 is the value of property P at time t_1, P_e is the equilibrium value of P at the final temperature, β is a constant ($0 \le \beta \le 1$), τ is a characteristic relaxation time expressed in the Narayanaswamy form,[15] and parameters β and τ together define the relaxation spectrum. In the Narayanaswamy expression (eq 2), A is a constant, Δh^* is a characteristic activation energy, X is a partitioning parameter ($0 \le X \le 1$) that separates Δh^* into two parts, characterizing temperature and structure dependence, respectively, R is the ideal gas constant; T is temperature, and T_f is the fictive temperature, a structural parameter. The Narayanaswamy expression has been extensively used to describe the temperature and structure dependence of τ[4,7-9,11,15,17-19] with great success, although there are other expressions, derived from the free volume concept[20] or the configurational entropy,[21] that have also been used successfully. Different expressions for τ have been enumerated, and the advantages of each of the expressions have been discussed in the literature.[1,10]

Fictive Temperature. Fictive temperature (T_f in eq 2) is a convenient concept for the description of the thermodynamic state of a glass and the progress of structural relaxation. According to Moynihan and coworkers,[4] the fictive temperature, T_f, of a given state is defined as "the temperature at which the equilibrium liquid has a relaxational value of P [a structure sensitive property] the same as that of the system in that state." An illustration of this definition is shown in Figure 1, where P and its temperature derivative, R, are shown as functions of temperature. The change in P caused by a change in temperature is divided into two parts, vibrational and relaxational. In the P–T diagram of Figure 1A the solid curve, which represents P as a function of temperature, shows a drastic change in slope in the glass transition region. Extrapolated values of P from the rubbery and the glassy states are shown by the dashed lines, whose intersection defines the fictive temperature (T_f). When the material is cooled from T_H to T, the relaxational part of the change in P in Figure 1A is represented by "I" and the vibrational part by "II" (or "II'" for a hypothetical cooling from T_H to T_f along the extrapolated rubbery state equilibrium line). The vibrational part of the change in P is characterized by a glasslike temperature dependence. To define the thermodynamic state of a glass at any given temperature, one must know the corresponding fictive temperature.

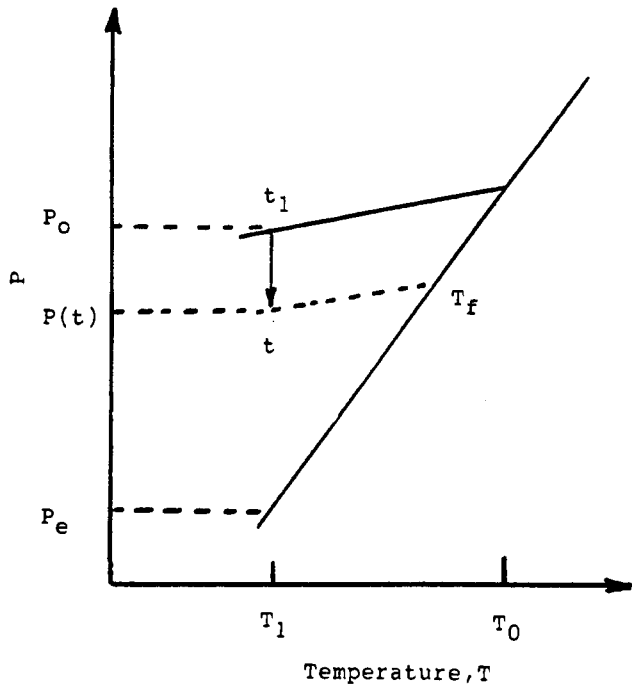

Figure 2. Schematic representation of relationship between relaxing property (P) and fictive temperature (T_f) after a temperature jump.

Mathematically, T_f is defined by

$$\int_T^{T_H} \frac{\partial(P-P_g)}{\partial T}\,dT = \int_{T_f}^{T_H} \frac{\partial(P_e-P_g)}{\partial T}\,dT \qquad (3a)$$

where P_e is the actual (or extrapolated) equilibrium value of P; P_g is the actual (or extrapolated) glassy state value of P; T is the temperature of the given state; T_H is a temperature in the rubbery state; and T_f is the fictive temperature. This definition is illustrated in the R–T diagram of Figure 1B. If one takes the derivative with respect to the temperature of both sides of eq 3a, an equivalent form, expressed in terms of R, the temperature derivative of P, is obtained:

$$dT_f/dT = [R(T) - R_g(T)]/[R_e(T_f) - R_g(T_f)] \qquad (3b)$$

In modeling of relaxation phenomena, fictive temperature serves the following two functions: (1) at constant pressure, the fictive temperature and the temperature of a glass together describe the thermodynamic state of the system, and (2) the temperature derivative of the fictive temperature corresponds to that of the relaxing property (as described in eq 3b) and provides a link between changes in the thermodynamic state and the property of the system. The second role is significant because, for a given set of thermal treatments, fictive temperature can be established as a function of temperature through model simulation (this point will be demonstrated later) and temperature derivatives of both the fictive temperature and the relaxing property can be conveniently obtained.

Structural Relaxation in Nonisothermal Conditions. In nonisothermal situations, structural relaxation can be described with equations derived from eq 1. By assuming the relaxation function to be linear with respect to temperature jumps, one can formulate the net response as the superposition of responses of the system to the series of temperature jumps that constitute the thermal history. The resulting equation is

$$T_f(T) = T_0 + \int_{T_0}^{T} dT'\{1 - \exp[-(\int_{t(T')}^{t(T)} dt/\tau)^\beta]\} \qquad (4)$$

where T_0 is the initial temperature.

In deriving eq 4, a relationship between the fictive temperature T_f and the value of P has been used. This relationship, as illustrated in Figure 2, describes the isothermal relaxation after a temperature jump from T_0 to T_1: a decrease in T_f occurs in proportion to the decrease in P. In terms of P and T_f, the normalized relaxation function ϕ is

$$\phi(t-t_1,t) = \frac{P-P_e}{P_0-P_e} = \frac{T_1-T_f(t)}{T_1-T_0} \qquad (5)$$

The simulated relaxation of P can be obtained by solving eqs 2 and 4 simultaneously.

The phenomenological model for structural relaxation composed of eqs 2 and 4 has been referred to as the Narayanaswamy model or, more frequently, the Moynihan model, although many other researchers have contributed to the development of this model.

Equations of the Moynihan Model in Discrete Form. The empirical kinetic equations of the Moynihan model (eqs 2 and 4) must be solved by numerical methods. To accommodate the discrete nature of numerical calculations, eqs 2 and 4 were rewritten as

$$T_f(m) = T_0 + \sum_{j=1}^{m} \Delta T(j)\{1 - \exp[-(\sum_{k=j}^{m} \Delta t(k)/\tau(k))^\beta]\} \qquad (6)$$

and

$$\tau(k) = A \exp[X\Delta h^*/(RT(k)) + (1-X)\Delta h^*/(RT_f(k))] \qquad (7)$$

where m is an iteration index and j and k are dumb indices. Caution must be exercised in that T_0, the starting temperture for the simulation, has to be sufficiently high so that the system is in equilibrium at that temperature. This restriction is necessary because properties of glasses are route dependent, and every step in the thermal history of the glass continues to influence its current properties. To accurately describe a glass in a nonequilibrium state, one must take into account the effect of every step along its route of transition after the last equilibrium state.

For simple thermal histories the conversion from continuous to discrete form can be performed in a straightforward manner. But when the thermal history contains both isothermal and rate-heating steps, it can become complicated. Our experiments involved a sequence consisting of a cooling step (from T_0 in the rubbery state to T_1 in the glassy state), an isothermal step (relaxation in the glassy state for a period t_e), and a heating step (from T_1 in the glassy state to T_0 in the rubbery state). Accordingly, the kinetic equations were rewritten as follows: (1) for the cooling step

$$T_f(m) = T_0 + \sum_{j=1}^{m} \Delta T(j)\{1 - \exp[-(\sum_{k=j}^{m} (\Delta T(k)/q(k))/\tau(k))^\beta]\} \qquad (8)$$

and $1 \le m \le IM$, (2) for the isothermal step

$$T_f(n) = T_0 + \sum_{j=1}^{m} \Delta T(j)\{1 - \exp[-(\sum_{k=j}^{m} (\Delta T(k)/q(k))/\tau(k) + \sum_{k=m+1}^{n} \Delta t(k)/\tau(k))^\beta]\} \qquad (9)$$

and IM ≤ n ≤ IN, (3) for the heating step

$$T_f(c) = T_0 + \sum_{j=1}^{m} \Delta T(j)\{1 - \exp[-(\sum_{k=j}^{m} (\Delta T(k)/q(k))/ \tau(k) + \sum_{k=m+1}^{n} \Delta t(k)/\tau(k) + \sum_{k=n+1}^{c} (\Delta T(k)/q(k))/\tau(k))^{\beta}]\} + \sum_{j=n+1}^{c} \Delta T(j)\{1 - \exp[-(\sum_{k=j}^{c} (\Delta T(k)/q(k))/\tau(k))^{\beta}]\} \quad (10)$$

and IN ≤ c ≤ IC, and (4) for all three steps

$$\tau(k) = A \exp[X\Delta h^*/(RT(k)) + (1 - X)\Delta h^*/(RT_f(k))] \quad (11)$$

In the above equations, m, n, and c are iteration indicies, j and k are dumb indicies, and IM, IN, and IC mark the last iterations in the cooling, isothermal, and heating steps, respectively. The values for IM, IN, and IC are determined by parameters T_0, T_1, t, $\Delta T(j)$, and $\Delta t(j)$. For example, if the temperature increments are uniform during cooling, i.e. $\Delta T = \Delta T(j)$, then IM = $(T_1 - T_0)/\Delta T$. In this example ΔT is negative as it should be for a cooling step. Finally, the derivative of the fictive temperature (T_f) with respect to temperature (T) at the ith interval during cooling or heating was approximated by

$$dT_f(i)/dT = (T_f(i + 1) - T_f(i))/(T(i + 1) - T(i)) \quad (12)$$

The simulation procedure was performed in the following manner. From eqs 8–11, we determined fictive temperature of the system as a function of thermal treatments. Next, from eq 12 we calculated the temperature derivative of T_f, which is related to the temperature derivative of the relaxing property as described by eq 3b. By doing so, we established a model capable of describing the time-dependent changes in properties of polymeric glasses and ready to be incorporated into simulation of structural relaxation.

Experimental Section

Materials. Both polymers used in this study are commercially available. PMMA was Plexiglas VS-100 from Rohm and Haas, a low T_g injection molding grade. Intrinsic viscosity of this polymers was found to be 0.37 dL/g at 25 °C in chloroform. SAN was Tyril-1000 natural from Dow Chemical, with acrylonitrile content of 25.3 wt % determined by the elemental analysis. The weight-average molecular weight of SAN was determined by gel permeation chromatography (GPC) and was found to be 150 000.

Sample Preparation. Blends of compositions ranging from 0 to 100 wt % SAN were prepared at 20 wt % intervals with a twin-screw extruder (courtesy of Werner-Pfleiderer Corp.). Before blending, resins were dried in a vacuum oven at 80 °C for 24 h.

Pellets of these blends were dried again and molded into $^1/_{16}$ in. thick sheets in a laboratory hot press. These sheets were then cut into small disks of about 10 mg each for enthalpy relaxation measurements and encapsulated hermetically in DSC aluminum pans. All samples were heated to 150 °C and held there for 15 min prior to testing to erase the effects of previous thermal history.

Thermal Analysis. A Perkin-Elmer differential scanning calorimeter, Model DSC-7, was used to perform the thermal analysis. The temperature scale and the energy output of the calorimeter were calibrated with the melting transition of indium. In addition, the power output scale was checked with a sapphire disk at temperatures ranging from 30 to 150 °C. Both calibrations were performed frequently. To ensure the same thermal treatment in all analyses, a cooling rate of 100 °C/min and a heating rate of 10 °C/min were applied in every case.

T_g's of the blends were measured and reported elsewhere.[13] The inflection point on the power output curve in the glass transition region was taken as the T_g. The T_g's were used as the reference temperature in choosing the aging temperatures for each blend composition. A single composition-dependent T_g is an indication of the miscibility of these polymers.

The Rate-Heating Approach. Specific heat of PMMA/SAN blends as a function of temperature in the glass transition region was measured. The specimen was first heated to 150 °C, then cooled to 30 °C at −100 °C/min, and, after the power output of DSC stabilized, heated to 150 °C at 10 °C/min. Thermogram obtained in the last step represents the C_p of the material through the glass transition region.

The Isothermal Approach. Three aging temperatures were used in this study with reference to the respective T_g of each blend: T_g − 20 °C, T_g − 35 °C, and T_g − 50 °C. The longest aging time was about 150 min at T_g − 20 °C and over 2000 min at T_g − 50 °C.

At the beginning of each run the specimen was heated to 150 °C and held there for 15 min to erase the effects of previous thermal history and then cooled to the desired aging temperature. The aging process took place in the DSC cell (in situ) for runs at T_g − 20 °C and T_g − 35 °C and in an oven for runs at T_g − 50 °C.

At the end of aging period, the specimen was cooled to 30 °C. Heating was initiated immediately after the thermal equilibrium was achieved at this lower temperature, usually in less than 2 minutes. The heating sequence consisted of an isothermal period at 30 °C, followed by a constant heating rate period leading to a temperature at about T_g + 40 °C and another isothermal period at that higher temperature. The specimen was then cooled to 30 °C, and the identical heating sequence was repeated immediately. This "reheat" run provided the unaged reference sample.

A run with an empty pan using the same isothermal–heating–isothermal sequence was performed beforehand, and the resulted thermogram was stored into the DSC control software as the base line, which was used as the reference for the recorded power output. The power output during each heating phase was recorded as a function of time.

Results and Discussion

Experimental results of enthalpy relaxation in PMMA/SAN blends were reported in our previous communication[13] and will be used but not repeated here. In this study we shall evaluate the consistency of the Moynihan model and describe its use in the simulation of enthalpy relaxation.

Specific Heat in the Transition Region. In the case of enthalpy relaxation, property P in the Moynihan model is the enthalpy, H, and its temperature derivative R, the specific heat, C_p. Specific heat is measured directly by DSC, and enthalpy is obtained by integration of specific heat with respect to temperature. The accuracy of C_p values in the glass transition region is crucial and was applied in this study as the criterion in determining the optimized parameters.

In the Moynihan model, the progress of enthalpy relaxation is expressed in terms of the change in fictive temperature. A new variable, the normalized specific heat, C_p^N, is defined to relate the changes in C_p and fictive temperature

$$C_p^N(T) = [C_p(T) - C_{pg}(T)]/[C_{pe}(T_f) - C_{pg}(T_f)] \quad (13)$$

C_p^N is equal to (dT_f/dT) in eq 3b and is a convenient variable for simulations using the Moynihan model.

To normalize the measured values of C_p, we have employed the following procedure. First, a numerical integration was performed on the C_p function to determine the T_f according to a modified form of eq 3a:

$$\int_T^{T_H} (C_p - C_{pg})\, dT = \int_{T_f}^{T_H} (C_{pe} - C_{pg})\, dT \quad (3a)$$

Then, the C_p was normalized according to eq 13.

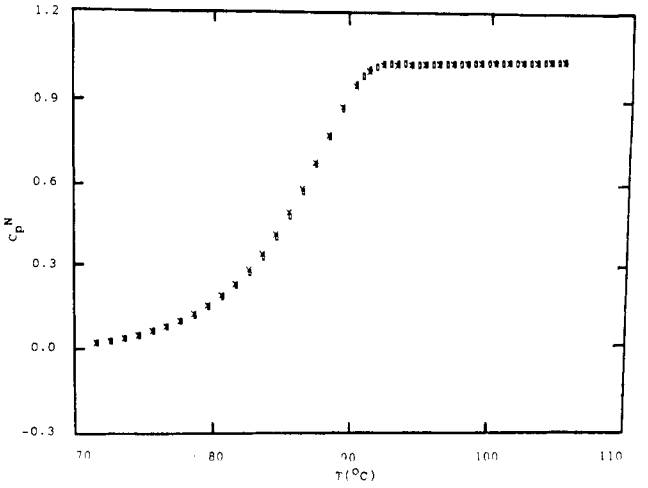

Figure 3. Effect of change in ΔT on C_p^N in the glass transition region: (□) ΔT = 0.5 K; (×) ΔT = 1.0 K. C_p^N values were calculated by using the Moynihan model with X = 0.4, β = 0.3, $\Delta h^*/R$ = 130 000 K, and ln A = −363.7.

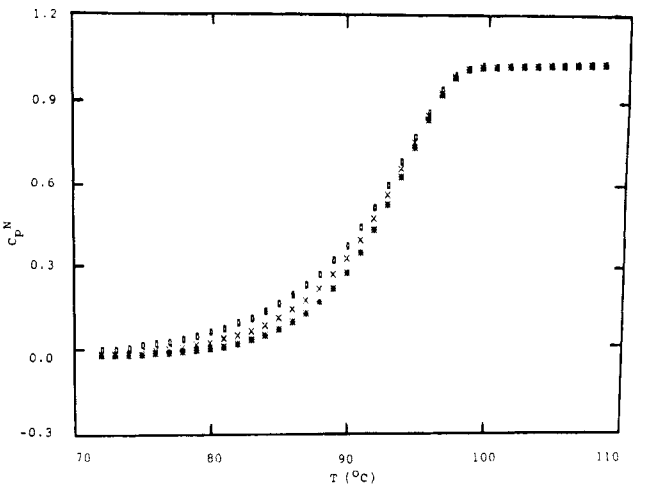

Figure 4. Effect of change in X on C_p^N in the glass transition region: (□) X = 0.3; (×) X = 0.4; (*) X = 0.5. C_p^N values were calculated by using the Moynihan model with β = 0.3, $\Delta h^*/R$ = 130 000 K, and ln A = −363.7.

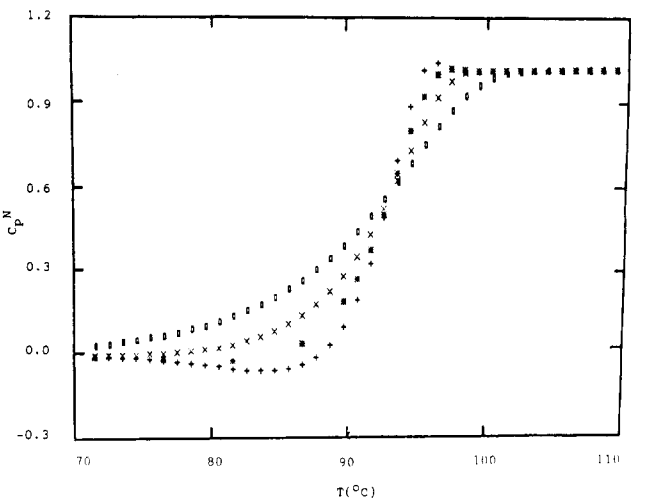

Figure 5. Effect of change in β on C_p^N in the glass transition region: (□) β = 0.2; (×) β = 0.3; (*) β = 0.4; (+) β = 0.5. C_p^N values were calculated by using the Moynihan model with X = 0.4, $\Delta h^*/R$ = 130 000 K, and ln A = −363.7.

Effects of Material Parameters on Calculated Specific Heat. We have used five adjustable parameters in the simulation of enthalpy relaxation with the Moynihan model; four of them (X, β, Δh^*, and A) are characteristics of the material (see eq 2), and the fifth one ($\Delta T(i)$) is used to vary the size of the temperature increment in the simulation of cooling or heating.

Parametric studies were carried out to examine the effect of variation in each of the adjustable parameters on the calculated results. The time increment in the isothermal step, a nonadjustable parameter, was set at one-tenth of a decade on the logarithmic time scale. This magnitude was chosen because the relaxation time tends to increase in proportion to the logarithm of the aging time. A uniform time increment based on the logarithmic time scale assures a proper weight for each segment of the isothermal step, and the proper balance is reflected in the uniform values for the $\Delta t(i)/\tau(i)$ terms. The other nonadjustable parameters in the simulation were set according to the experimental conditions, namely, T_0 = 150 °C, T_1 = 30 °C, t_e = 5 min, Q_c = −100 °C/min, and Q_h = 10 °C/min.

For polymers, values for parameters X, β, $\Delta h^*/R$, and ln A have been reported.[10] The simulation was initiated by choosing the following value for each parameter from the range reported in the literature: X = 0.400, β = 0.300, $\Delta h^*/R$ = 132.6 × 10^3 K, and ln A = −363.7.

The parametric study was carried out by varying one of the parameters while keeping the others constant and thus evaluating its effect on the calculated values of specific heat. The effect of varying ΔT was examined by comparing the results obtained with two different values of ΔT, 0.5 and 1.0 K. For convenience, the same temperature increment was used in simulations of both cooling and heating, i.e. $\Delta T = \Delta T_{heating}(i) = -\Delta T_{cooling}(i)$. In Figure 3, C_p^N (defined by eq 3b or 13) is plotted as a function of temperature. As seen in this figure, there is only negligible difference between data obtained with ΔT = 1.0 K and ΔT = 0.5 K; however, the former required much less time for computation and was therefore used in all calculations.

Three levels of X, 0.3, 0.4, and 0.5, were examined next. As shown in Figure 4, an increase in X shifts the inception of the transition to a higher temperature but affects little the upper bound of the glass transition region. As a results, the transition region becomes narrower with increasing X.

Table I
Moynihan Model Parameters for a Series of PMMA/SAN Blends

	compositn, wt % SAN					
	100	80	60	40	20	0
X	0.221	0.137	0.147	0.253	0.227	0.338
β	0.482	0.460	0.423	0.346	0.351	0.265
$\Delta h^*/R$/1000 K	125.0	134.7	138.6	146.2	140.3	132.2
ln A	−328.9	−358.5	−370.8	−392.6	−377.6	−359.8

Among the four material parameters, change in β results in the most prominent variation in the shape of the C_p^N curve in the transition region. As shown in Figure 5, as low β value (e.g. (0.2) produces a broad transition but no pre-transition dip or post-transition overshoot. On the other hand, a high β value (>0.4) leads to a very narrow transition with both pre-transition dip and post-transition overshoot.

In Figure 6, calculated results with two levels of $\Delta h^*/R$, 132.6 × 10^3 and 130.0 × 10^3 K, are presented. A third curve obtained by shifting the lower $\Delta h^*/R$ curve to the right along the temperature scale is also shown. It is clearly seen in this figure that the third curve overlaps the higher

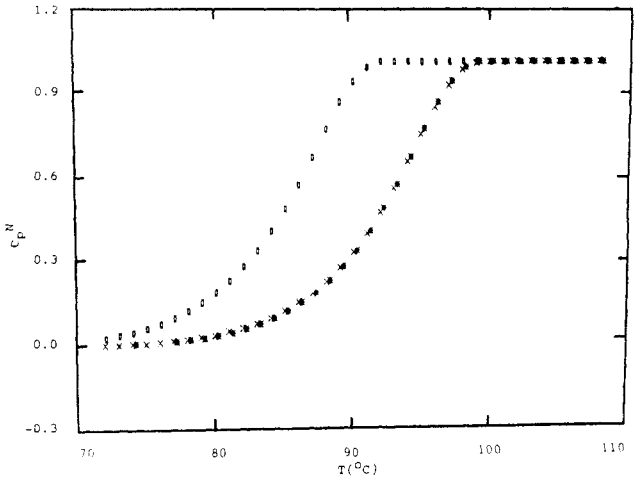

Figure 6. Effect of change in $\Delta h^*/R$ on C_p^N in the glass transition region: (□) $\Delta h^*/R$ = 130 000 K; (×) $\Delta h^*/R$ = 132 600 K; (*) $\Delta h^*/R$ = 130 000 K (shifted). C_p^N values were calculated using the Moynihan model with X = 0.4, β = 0.3, and ln A = −363.7.

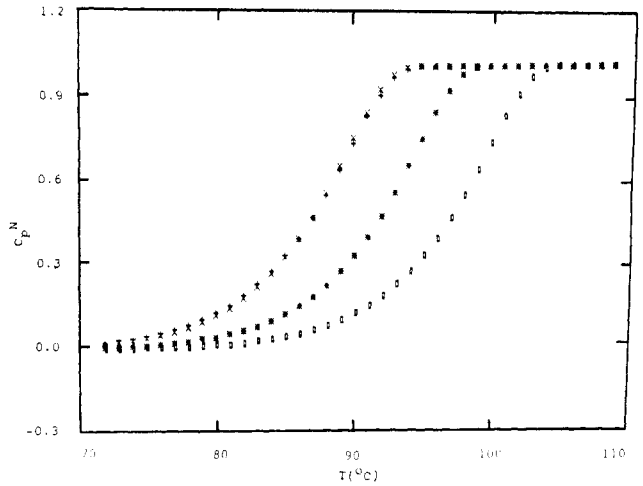

Figure 7. Effect of change in ln A on C_p^N in the glass transition region: (□) ln A = −358.7; (×) ln A = −363.7; (*) ln A = −368.7; (+) ln A = −358.7 (shifted). C_p^N values were calculated by using the Moynihan model with X = 0.4, β = 0.3, and $\Delta h^*/R$ = 130 000 K.

$\Delta h^*/R$ curve. From this observation, it can be concluded that the effect of change in $\Delta h^*/R$ is to shift the C_p^N curve along the temperature scale without affecting its shape.

Similar effect was also observed when ln A was varied. In Figure 7, data obtained for three values of ln A, −358.7, −363.7, and −368.7, are plotted. Again the curves can be horizontally shifted to superimpose upon one another.

In Figures 4–7, we have summarized the effects of variation of each adjustable parameter on the calculated specific heat. This knowledge is essential for the proper choice of starting parameters for optimization, as will be illustrated in the following sections.

Optimized Parameters from the Rate-Heating Approach. Optimized Moynihan parameters for each composition were obtained in the simulation of experments following the rate-heating approach. In these experiments, a material is cooled from the rubbery state to the glassy state and reheated back to the rubbery state immediately. The goal of the optimization was to find the set of parameters that best describes the behavior of the C_p of the material in the glass transition region. The objective function for the optimization was therefore $\sum(C_p^{N*} - C_p^N)^2$, where C_p^{N*} is the calculated value for the normalized specific heat in the transition region and C_p^N its experimentally obtained counterpart. Optimization was carried out by using the Marquardt algorithm given by Kuester and Mize,[22] which, with a proper choice of starting values, converges expeditiously in situations involving nonlinear equations with multiple variables. The computer codes were written in Fortran language and could be accommodated and executed in a personal computer.[23]

We began our optimization process by obtaining a set of starting values for 100% PMMA through a procedure similar to that used by Hodge and co-workers[6-10] in their studies of enthalpy relaxation in organic glasses. We determined the starting values for the parameters in the following way:

1. $\Delta h^*/R$ was obtained experimentally from the dependence of T_f on the cooling rate Q_c:

$$\Delta h^*/R = -\mathrm{d} \ln Q_c / \mathrm{d}(1/T_f) \quad (14)$$

2. ln A was determined from eq 2 by assuming that at the glass transition temperature τ is of the order of 1 min and $T = T_f (= T_g)$. With $\Delta h^*/R$ obtained in step 1, ln A was calculated from

$$\ln A = \Delta h^*/(RT_g) \quad (15)$$

3. X and β were chosen to be in agreement with literature values reported by many researchers.[1,5-10]

A preliminary calculation of the C_p^N was then performed with these values, and the results were compared with the experimental data by plotting both on a video monitor. Additional fine tuning was required when the two sets of data did not match in the video image. To improve the matching, the parameters were adjusted. The adjustments were done in accordance with the observed effect of each parameter on the calculated C_p^N values, shown in Figures 4–7. We recall that changes in ln A and $\Delta h^*/R$ shift the curve horizontally and changes in X and β modify the shape of the curve. When satisfactory matching was recorded in the video image, that particular set of parameters was defined and used as input for optimization.

The optimized parameters were usually arrived at after about five iterations, but because of the repetitive nature of the calculation, it takes 2–3 h to perform calculations in a personal computer.

The optimized parameters for 100% PMMA were then used as the starting values for the next blend in the series, i.e., the PMMA/SAN 80/20 blend, and the above described optimization process was repeated. By iterating the process, the optimized parameters were generated for each blend. These parameters are tabulated in Table I.

A comparison of experimental and calculated results for C_p^N as a function of temperature and blend composition is shown in Figure 8A–F. As seen in these plots, the model accurately indicates the position and the width of the glass transition region as well as the position of the post-transition peak for all compositions, but it underestimates its intensity in most cases. For example, for PMMA/SAN 80/20 blend (Figure 8B), where the most severe discrepancy occurs, the model underestimates the normalized C_p by about 5% for a zone of about 5 °C, although the average discrepancy over the transition region is within the experimental uncertainty (0.3% for C_p).

Simulation of the Isothermal Approach. We then proceeded to simulate the isothermal relaxation by using the optimized parameters for each composition listed in Table I. The simulated route was designed to match as closely as possible the experimental conditions, which con-

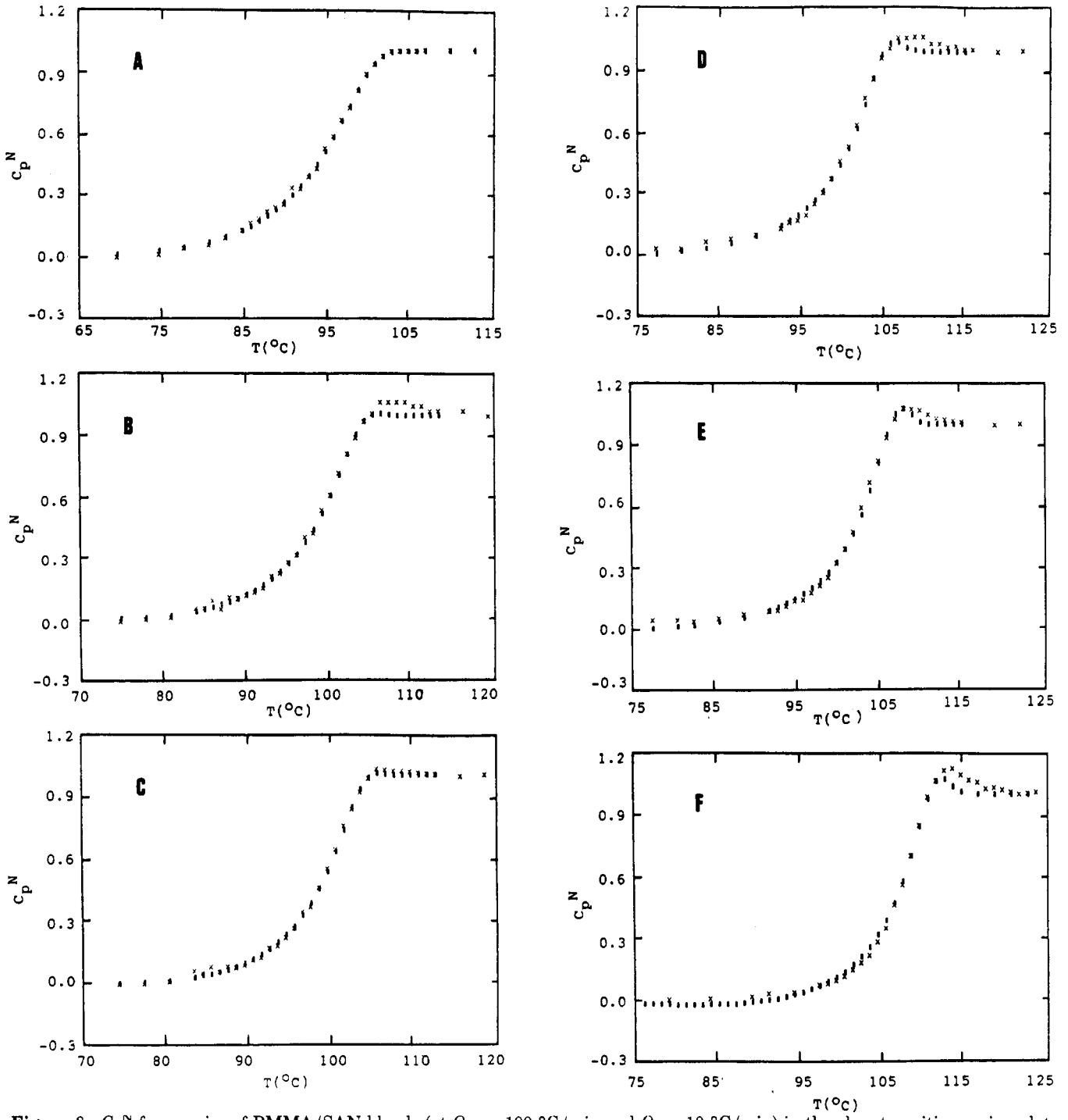

Figure 8. C_p^N for a series of PMMA/SAN blends (at Q_c = −100 °C/min and Q_h = 10 °C/min) in the glass transition region plotted as a function of temperature: (□) experimental; (×) calculated. The calculated values were obtained by using the Moynihan model with parameters listed in Table I: plot A, 100% PMMA by weight; plot B, 80%; plot C, 60%; plot D, 40%; plot E, 20%, and plot F, 0%.

sisted of three steps: a rapid cooling step from a temperature (T_H) above T_g to the aging temperature, T_A, at a rate of −100 °C/min; an isothermal period at T_A for a duration t_e; and a heating step from T_A to T_H at a rate of 10 °C/min. Three levels of T_A, T_g − 20, T_g − − 5, and T_g − 50 °C, were employed, and the duration of the isothermal period, t_e, varied from zero to 2000 min.

Numerical integration of the calculated values of C_p with respect to temperature was performed along the heating step from T_A to T_H. The obtained result represents the difference in enthalpy between the equilibrium state at T_H and the aged state at T_A with an isothermal aging time t_e. For clarity, we shall call this quantity $\Delta H(t_e,T_A)$. An additional integration was performed on the actual (or extrapolated) equilibrium C_p function over the same range, the result of which is the extrapolated difference in enthalpy between equilibrium states at T_A and T_H. We shall call this quantity $\Delta H_e(T_A)$. A new variable $\phi(t_e,T_A)$ was then defined as

$$\phi(t_e,T_A) = [\Delta H_e(T_A) - \Delta H(t_e,T_A)]/[\Delta H_e(T_A) - \Delta H(0,T_A)] \quad (16)$$

And ϕ is a measure of the extent of enthalpy relaxation.

In Figure 9A–F, ϕ is plotted as a function of aging time and aging temperature for various blend compositions. The discrete symbols represent experimental values determined as described in our previous publication,[13] and the

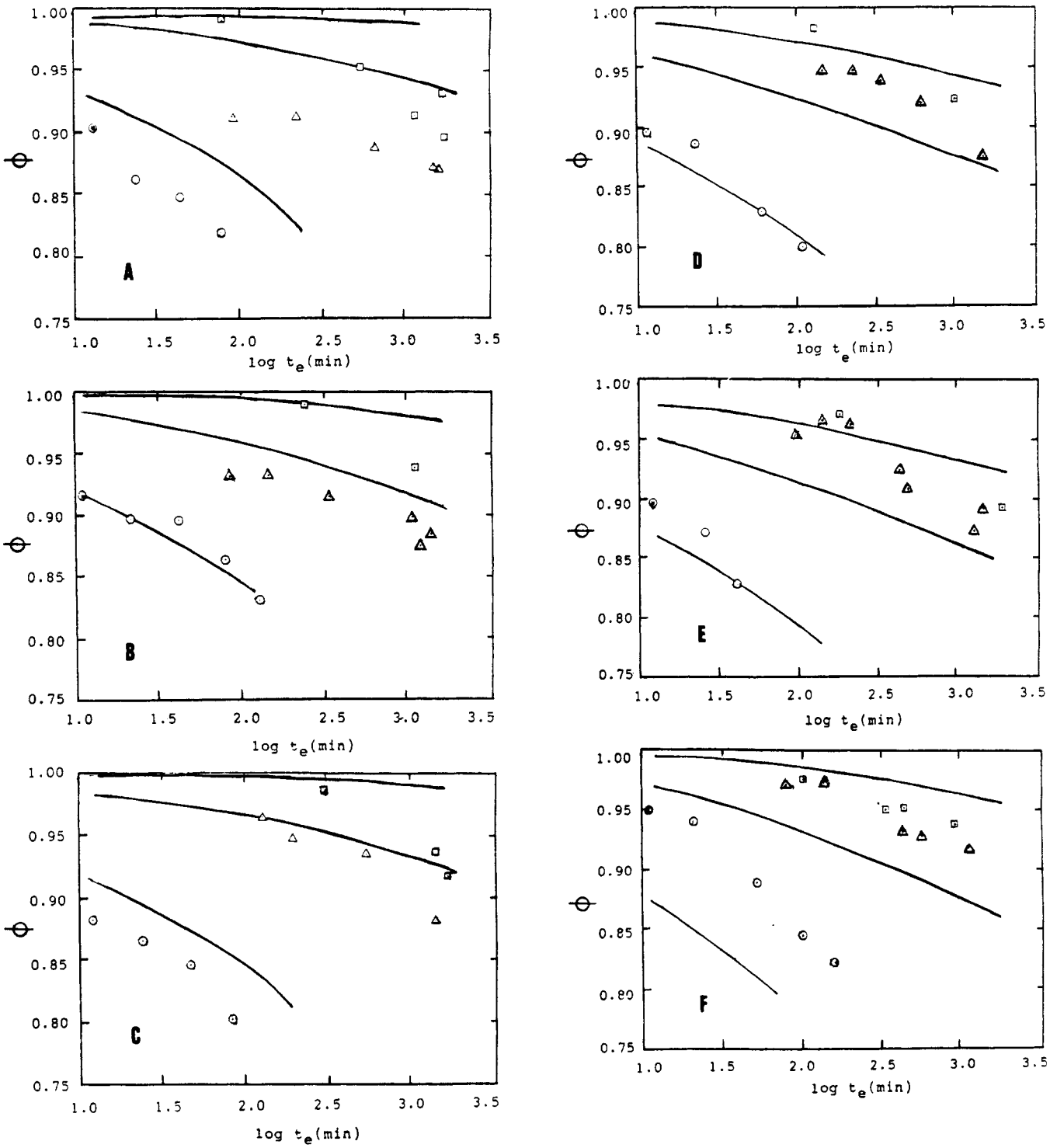

Figure 9. Enthalpy relaxation of a series of PMMA/SAN blends plotted as a function of aging time. Data were obtained at (⊡) T_g - 50 °C, (△) T_g - 35 °C, and (⊙) T_g - 20 °C. Solid curves represent calculated values obtained by using the Moynihan model with parameters listed in Table I: plot A, 100% PMMA by weight; plot B, 80%; plot C, 60%; plot D, 40%; plot E, 20%; and plot F, 0%.

solid curves represent the results obtained with the Moynihan model at three different temperatures (from top to bottom, T_g - 50, T_g - 35, and T_g - 20 °C).

The accuracy of the Moynihan model in describing isothermal enthalpy relaxation should be assessed considering the uncertainty associated with the experimental data. There are two kinds of indeterminate errors that might be associated with our experimental data; constant errors caused by the measuring instrumentation and accidental errors caused by fortuitous variations in the sensitivity of measuring instruments.[24] Effects of accidental errors on our results have been addressed previously,[13] and the maximum uncertainty in ϕ values incurred from this source has been estimated at 4%.

Daily variation in DSC calibration curves obtained with either an empty sample pan or a standard sapphire specimen has been noticed in our laboratory and can be attributed to the effects of changing ambient humidity. (Although the two sample cells in DSC are purged with dry nitrogen gas, the aluminum block surrounding the cells, serving as the heat sink, is in contact with the absorbent-dry air. Water condensation, which is a function of ambient humidity, always occurs on the surface of the aluminum block and could interfere in its function as

the heat sink.) The variation in power output becomes clear especially at temperatures higher than 100 °C, reaching 2% at 140 °C, and is a constant error in character. For PMMA/SAN blends, the lower limit of the rubbery state coincides with the temperature region of high DSC output variation, and the extrapolated C_p values from the rubbery state are susceptible to this constant error. Extrapolated C_p values are used in the calculation of the equilibrium enthalpy at the aging temperature, which therefore is also affected by the constant error. The effects of the constant error are carried over to the phi value through calculations. On the basis of the knowledge that at 140 °C the uncertainty of the DSC power output is about 2%, we have estimated that, besides the 4% uncertainty in the experimental ϕ values due to the accidental errors, additional uncertainty varying from 1.5% (at T_g - 20 °C) to 4.3% (at T_g - 50 °C) is caused by the constant error.

In light of the above discussions, the agreement between experimental and calculated values shown in Figure 9 is actually very good, with observed discrepancies within the maximum experimental uncertainty. We thus maintain that the observed agreement between experimental and calculated results provides evidence for the consistency of the Moynihan model in describing enthalpy relaxation of polymer blends.

Conclusions

By comparing simulated enthalpy relaxation behavior of a series of PMMA/SAN blends, calculated by using the Moynihan model, with experimental data, the following major conclusions have been reached.

The Moynihan model describes enthalpy relaxation in the glassy state quite well. Calculated specific heat function in the rate heating approach and calculated isothermal enthalpy relaxation in the isothermal approach were both found to be in good agreement with experimental data.

The kinetic theories of the glass transition, upon which the Moynihan and other models of that genre were built, are essentially correct in describing both the transition and the glassy region by accounting for the effects of temperature and structure on enthalpy relaxation.

Acknowledgment. This material is based upon work supported by the National Science Foundation under Materials Research Group (MRG) Grant No. DMR-8508084.

References and Notes

(1) Sherer, G. *Relaxation in Glass and Composites*; Wiley: New York, 1986.
(2) Kovacs, A. J. *J. Polym. Sci.* **1958**, *30*, 131.
(3) Kovacs, A. J. *Adv. Polym. Sci.* **1963**, *3*, 394.
(4) Moynihan, C. T.; Easteal, A. J.; DeBolt, M. A.; Tucker, J. *J. Am. Ceram. Soc.* **1976**, *59*, 12.
(5) DeBolt, M. A.; Easteal, A. J.; Macedo, P. B.; Moynihan, C. T. *J. Am. Ceram. Soc.* **1976**, *59*, 16.
(6) Berens, A. R.; Hodge, I. M. *Macromolecules* **1982**, *15*, 756.
(7) Hodge, I. M.; Berens, A. R. *Macromolecules* **1982**, *15*, 762.
(8) Hodge, I. M.; Huvard, G. S. *Macromolecules* **1983**, *16*, 371.
(9) Hodge, I. M. *Macromolecules* **1983**, *16*, 898.
(10) Hodge, I. M.; *Macromolecules* **1987**, *20*, 2897.
(11) Kovacs, A. J.; Aklonis, J. J.; Hutchinson, J. M.; Ramos, A. R. *J. Polym. Sci., Polym. Phys. Ed.* **1979**, *17*, 1097.
(12) Struik, L. C. E. *Polymer* **1988**, *29*, 1347.
(13) Mijovic, J.; Ho, T.; Kwei, T. K. *Polym. Sci. Eng.* **1989**, *29*, 1604.
(14) Hutchinson, J. M.; Kovacs, A. J. *J. Polym. Sci., Polym. Phys. Ed.* **1976**, *14*, 1575.
(15) Narayanaswamy, O. S. *J. Am. Ceram. Soc.* **1971**, *54*, 491.
(16) Williams, G.; Watts, D. C. *Trans. Faraday Soc.* **1970**, *66*, 80.
(17) Tool, A. Q. *J. Am. Ceram. Soc.* **1946**, *29*, 240.
(18) Ritland, H. N. *J. Am. Ceram. Soc.* **1956**, *39*, 403.
(19) Mazurin, O. V.; Rekhson, S. M.; Startsev, Y. K. *Sov. J. Glass Phy. Chem. (Engl. Transl.)* **1975**, *5*, 412.
(20) Macedo, P. B.; Litovitz, T. A. *J. Chem. Phys.* **1965**, *62*, 245.
(21) Adam, G.; Gibbs, J. H. *J. Chem. Phys.* **1965**, *43*, 139.
(22) Kuester, J. L.; Mize, J. H. *Optimization Techniches with Fortran*; McGraw-Hill: New York, 1973.
(23) Ho, T. Ph.D. Thesis, Polytechnic University, **1990**.
(24) Mickley, H. S. *Applied Mathematics in Chemical Engineering*; 2nd ed.; McGraw-Hill: New York, 1957.

Registry No. Plexiglass VS-100, 9010-88-2; SAN, 9003-54-7.